

UC Irvine

UC Irvine Previously Published Works

Title

Stimulated blue emission in reconstituted films of ultrasmall silicon nanoparticles

Permalink

<https://escholarship.org/uc/item/9t8066j8>

Journal

Applied Physics Letters, 78(8)

ISSN

0003-6951

Authors

Nayfeh, MH
Barry, N
Therrien, J
[et al.](#)

Publication Date

2001-02-19

DOI

10.1063/1.1347398

Copyright Information

This work is made available under the terms of a Creative Commons Attribution License, available at <https://creativecommons.org/licenses/by/4.0/>

Peer reviewed

Stimulated blue emission in reconstituted films of ultrasmall silicon nanoparticles

M. H. Nayfeh,^{a)} N. Barry, J. Therrien, O. Akcakir, E. Gratton, and G. Belomoin

Department of Physics, University of Illinois at Urbana-Champaign, 1110 West Green Street, Urbana, Illinois 61801

(Received 12 July 2000; accepted for publication 14 December 2000)

We dispersed electrochemical etched Si into a colloid of ultrabright blue luminescent nanoparticles (1 nm in diameter) and reconstituted it into films or microcrystallites. When the film is excited by a near-infrared two-photon process at 780 nm, the emission exhibits a sharp threshold near 10^6 W/cm², rising by many orders of magnitude, beyond which a low power dependence sets in. Under some conditions, spontaneous recrystallization forms crystals of smooth shape from which we observe collimated beam emission, pointing to very large gain coefficients. The results are discussed in terms of population inversion, produced by quantum tunneling or/and thermal activation, and stimulated emission in the quantum confinement-engineered Si-Si phase found only on ultrasmall Si nanoparticles. The Si-Si phase model provides gain coefficients as large as 10^3 – 10^5 cm⁻¹. © 2001 American Institute of Physics. [DOI: 10.1063/1.1347398]

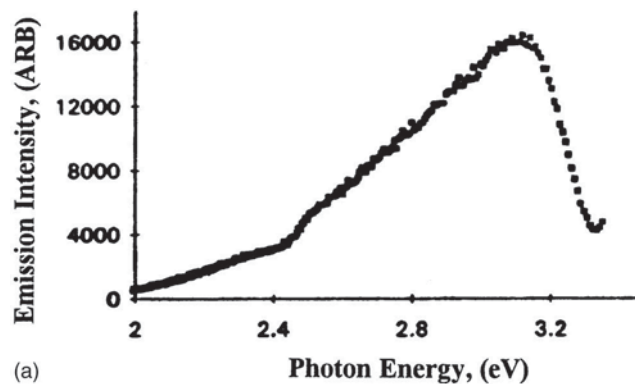
The discovery in 1990 of visible red luminescence by Canham and co-workers^{1,2} in electrochemical etched Si surprised the scientific community, since Si is an indirect gap material. Recently, we demonstrated another surprising effect of the presence of micron-size regions that are rich in ultrasmall structures, and for which the intensity of the luminescence has a sharp threshold near an average intensity of 10^6 W/cm², with highly nonlinear characteristics, rising by several orders under two-photon femtosecond excitation.³ At the threshold there is a dramatic increase in the slope of the power pumping curve from ~ 1.6 to ~ 11 – 12 , similar to stimulated emission in inverted systems. The region that exhibits the threshold behavior³ is abundant, but it is spotty, shallow, and uncontrollable. In this letter, we enriched the ultrasmall structure, dispersed it into a suspension colloid of ~ 1 nm diameter particles,⁴ and reconstituted it into large, thick, uniform, and under control films or microcrystallites on device quality Si or glass substrates. Under excitation with 355 nm, the luminescence of the colloid and the film are dominated by blue emission at ~ 390 nm, and is observable with the naked eye in room light. The brightness is high such that emission from a single particle is readily detectable.⁵ Two-photon excitation at 780 nm produces blue light, from all over the film, with a sharp threshold beyond which a low order power dependence that may saturate at the highest incident intensity sets in. Moreover, under some conditions, smooth crystals produce collimated beam emission. The results are discussed in terms of stimulated emission in the quantum confinement-induced Si-Si phase found only on ultrasmall Si particles.^{6,7} Under certain conditions of crystallization, the second harmonic, forbidden in bulk due to the centrosymmetry, was recently observed.⁸

(100) oriented, 1–10 Ω cm resistivity, *p*-type boron doped silicon was laterally anodized in H₂O₂ and HF.⁹ The peroxide catalyzes etching and cleans, resulting in much reduced substructures of high chemical and electronic quali-

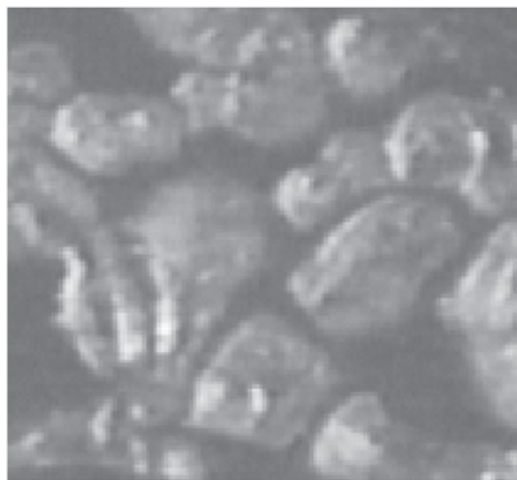
ties. The brighter spots are found where the current concentrates, such as in the meniscus (air-liquid interface).¹⁰ We advance the wafer at a speed of ~ 1 mm per hour to produce a large meniscus-like area. A subsequent ultrasound bath crumbles the film into ultrasmall particles. Transmission electron microscopy shows a size of 1 nm in diameter. Electron photospectroscopy shows that the particles are silicon with less than 10% oxygen. We then precipitated the particles into a thin film on Si or glass substrates. Figure 1(a) gives the emission spectrum of the film under excitation with 355 nm UV radiation, showing the blue band at 390 nm. Optical imaging [see Fig. 1(b)] shows, in some cases, smooth colloidal crystals of 10–50 μ m across. We used Ti-sapphire laser (150 fs pulses, 80 MHz rep rate). The average power, 5–300 mW, is focused to diffraction limited spot ~ 1 μ m diameter, giving an average (or cw) intensity of 2×10^5 – 4×10^7 W/cm² (peak intensity of 2×10^{10} – 4×10^{12} W/cm²). The interaction is viewed via an optical microscope ($\times 10$) and the excitation beam was raster scanned. Emission is detected by a photomultiplier and stored in a two dimensional array. The film emits, as seen by the naked eye, 1 μ m spot of intense “white blue” light. At high intensities, the sample may be damaged.

Figure 2 gives the emission intensity as a function of the average incident intensity. For low intensity, the emission is finite, but at $\sim 10^6$ W/cm², it exhibits a sharp threshold, rising by several orders of magnitude. Beyond the threshold, there sets in a low order power dependence that may saturate. There are several types of spatial profiles. When the incident beam is raster scanned in an irregularly shaped cluster region, nondirected intense flashes larger than the interaction spot may occasionally be observed. In the crystallites region, the spatial profile of the emission depends sensitively on the shape of the crystallite. Under some conditions of recrystallization, crystals of smooth shape may form. Figure 3 displays the interaction with this type of crystallite. The excitation beam, focused to 1 μ m spot, is normally incident (normal to the figure). The boundaries of the crystallites in

^{a)}Electronic mail: m-nayfeh@uiuc.edu



(a)



(b)

FIG. 1. (a) the emission spectrum from a reconstituted film of nanoparticles under excitation with 355 nm radiation. (b) A $100\ \mu\text{m} \times 100\ \mu\text{m}$ optical image of the film showing crystals of $5\text{--}20\ \mu\text{m}$ across.

Fig. 3 are not fully visible, because the images were taken with no white light. The images show that directed blue beams emerge from the interaction spot. These appear when the surface of the crystallite is concave. The beams, in some cases, get narrower before they fade away. If the outer portion is diverging, then under strong absorption it will disappear first making the beams appear collimated. Figure 4 shows the case where the opposite faces of a crystallite are cylindrical and close (boundaries not visible) and the generated beam strikes the opposite face, making a weaker bright spot. When the incident intensity is reduced the beam fades

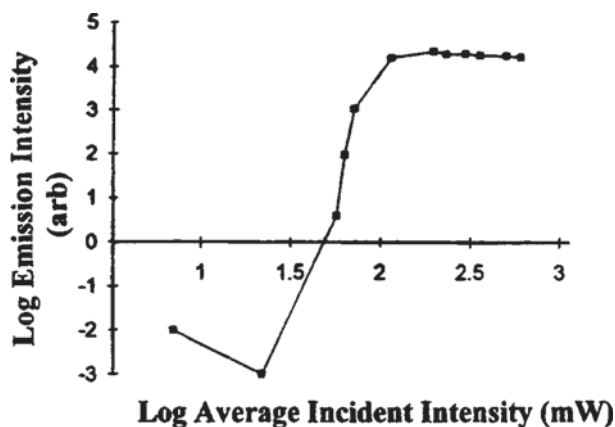


FIG. 2. Emission intensity as a function of the average incident intensity for a reconstituted thin film of Si nanoparticles.

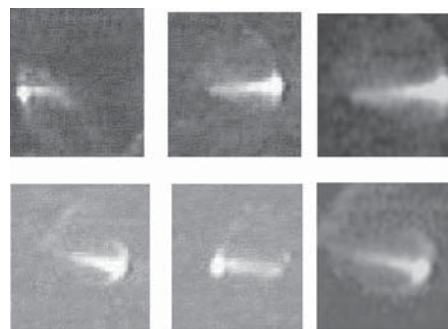


FIG. 3. Photoluminescence from the microcrystallite. The excitation beam, focused to a $1\ \mu\text{m}$ spot is normally incident (normal to the plane of the figure). The interaction spot appears as “white blue” spot. $20\ \mu\text{m} \times 20\ \mu\text{m}$ images showing examples of a blue beam. The beam is in the plane of the sample (normal to the incident beam), propagating in the interior of the crystallite, locally normal to its side.

away and disappears while the interaction spot remains bright pointing to a threshold as shown in Fig. 4. The blue beam is favored when the incident beam strikes close to a face of the microcrystallites, often quitting when it is moved to the interior, pointing to a need for large feedback by reflection. We observe divergent beam profiles when the crystallite faces are plane. In some cases, the size grows $5\ \mu\text{m}$ over $20\ \mu\text{m}$ of propagation, giving roughly a divergence of $125\ \text{mrad}$.

We now discuss systems that provide population inversion. A recent model^{6,7} demonstrated strong variations in the absorption and emission pathways with size, in the ultrasmall regime. Allan *et al.*⁶ theoretically discovered formation in ultrasmall nanocrystallites ($<1.75\ \text{nm}$) of new stable configuration (or phase) distinct from but interconnected to, a diamond-like structure by a potential barrier. It is based on the pairing of surface atoms to form intrinsic Si–Si dimer bonds. Figure 5 gives the interatomic potential of the bond⁶ and the various pathways for absorption and emission in a $1.03\ \text{nm}$ diameter particle.⁷ The excited state is a double well with a potential barrier where the outer well, a trap well (at $3.85\ \text{\AA}$) radiates with life times of $5\ \text{ns}\text{--}100\ \mu\text{s}$ while the inner well (at $2.35\ \text{\AA}$) radiates on a much longer time scale (ms). The state to which the outer well radiates is the ground state, high lying and unpopulated, hence this system constitutes a stimulated emission channel.

Direct excitation to the outer well is not allowed because transitions proceed vertically according to the Frank–Condon principle. But absorption proceeds into the inner well at a bond of $2.35\ \text{\AA}$, followed by transfer into the outer well by bond expansion via tunneling (double well vibrations) or thermal activation.^{6,7} Also, above-barrier absorption, followed by relaxation, populates the trapping well. For sizes less than a critical size of $\sim 1.4\ \text{nm}$ the trapping edge is lower than the absorption edge allowing stabilization of the outer well.⁷ Evidence for a potential-based state was demonstrated by manipulation with metal and oxide coatings.¹¹ Blue emission at $\sim 400\ \text{nm}$ is expected from radiative processes at the top of the barrier (at $\sim 3\ \text{\AA}$ bond length), with a short lifetime (submicron/nanosecond). The Si–Si produces gain from the bottom of the outer well; however, it is a smaller gain since the lifetime is in the μs regime. Measurements of the dispersed colloid particles gave life times of 1 ,

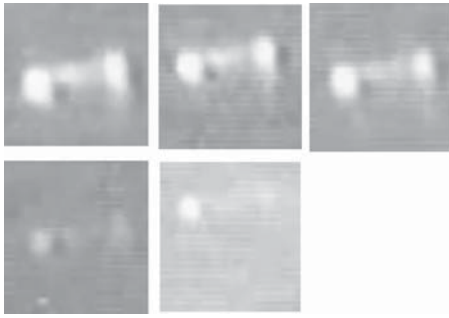


FIG. 4. $12\ \mu\text{m} \times 12\ \mu\text{m}$ photoluminescence images from the microcrystal-lites region, showing a blue beam between opposite faces, under decreasing incident intensity starting left to right, top to bottom.

5, 10–15 ns, and $\sim 100\ \mu\text{s}$, with most of the blue emission being in the 10–15 ns time scale, and the weak red component being in the μs regime.

The initial gain coefficient¹² is $\gamma = \Delta N \lambda^2 \Delta v / (8 \pi n^2 \tau)$ where ΔN is the population inversion, n is the refractive index, Δv is the emission width, λ is the wavelength, and τ is spontaneous lifetime. With near saturated absorption, followed by strong transfer, we expect the density of the excited emitters to be $\sim 25\%$ of the atomic solid density ($\sim 1.5 \times 10^{22}/\text{cm}^3$). Using $\tau = 0.01 - 1\ \mu\text{s}$, $\lambda = 400\ \text{nm}$, $n = 2$, and $\Delta v = 100\ \text{nm}$, we get $\gamma \sim 1.5 \times 10^3 - 1.5 \times 10^5\ \text{cm}^{-1}$. This gain allows considerable growth over microscopic distances. The number of spontaneous modes $p = 8 \pi \Delta v n^3 V / \lambda^2 c$, where V is the active volume. Using an active cross section and thickness of $(2\ \mu\text{m})^2$ and $0.2\ \mu\text{m}$, we get $p \sim 10^3$, sizable even for microscopic volume. Appreciable population ($\sim 50\%$) at the powers used requires a reasonable two-photon “cross section” $\beta \sim 10^{-46}\ \text{cm}^4$,³ with an absorption rate $R = \beta F^2$, where F incident photons/ $\text{cm}^2\ \text{s}$.

Koyama and Fauchet (KF)¹³ recently reported superlinear emission in porous Si in the infrared (600–1300 nm) with long ($> 10\ \text{ms}$) time scale. The samples must first be oxidized at 800–1000 °C. Emission is, however, quenched by attaching to a higher thermal conductivity substrate or by blowing air; thus it was attributed to heat effects. Our emission is in the blue ($\sim 400\ \text{nm}$) with a short time scale (10 ns). The particles are not heated or oxidized, and Fourier transform infrared and electron photo spectroscopy (EPS) show that they are hydrogen terminated. The emission is stable and blowing air does not quench it, whether the film is free standing, on glass, or on silicon substrates, and it is observed in the solid precursor, dispersed particles, or microcrystal-lites. The emission from single particles is already ultrabright and readily detectable.⁵ Finally, unlike KF, we observe collimated laser beam emission. We examined the time behavior. Operating the laser in cw mode, only the bright patches in the solid precursor respond. Moreover, dispersed particles are extremely dim but the films are ultrabright and exhibit a threshold. In the pulsed case the regions away from the bright patches fluoresce and dispersed particles are ultrabright. Since the average incident power is the same it is doubtful that the process is simply due to heat. In the dimer phase, thermal activation is a means for population but it is not the basic mechanism.⁷

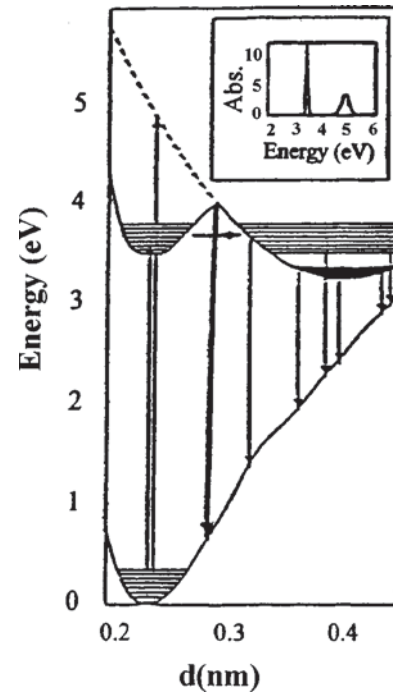


FIG. 5. The interatomic potential of the electronic ground state and first excited state of the Si–Si bond in a 1.03 nm diameter nanoparticles calculated by Allan *et al.* (Ref. 6) and the various pathways for absorption (vertical upward arrows) and emission (vertical downward arrows). The inset is the calculated absorption (Ref. 7).

In conclusion, we reported very sharp emission thresholds and directed, nondiverging blue beams in microcrystal-lites of ultrasmall Si nanoparticles. We discussed the results in terms of population inversion/stimulated emission in the confinement-induced Si–Si dimer phase predicted only on the ultrasmall particles.

The authors acknowledge State of Illinois Grant IDCCA No. 00-49106, US Department of Energy Grant No. DEFG02-91-ER45439, and NIH RR03155.

¹L. T. Canham, *Appl. Phys. Lett.* **57**, 1046 (1990).

²See for example; A. G. Cullis, L. T. Canham, and P. Calcott, *J. Appl. Phys.* **82**, 909 (1997).

³M. Nayfeh, O. Akcakir, J. Therrien, Z. Yamani, N. Barry, W. Yu, and E. Gratton, *Appl. Phys. Lett.* **75**, 4112 (1999).

⁴G. Belomoin, J. Therrien, and M. Nayfeh, *Appl. Phys. Lett.* **77**, 779 (2000).

⁵O. Akcakir, J. Therrien, G. Belomoin, N. Barry, E. Gratton, and M. Nayfeh, *Appl. Phys. Lett.* **76**, 1857 (2000).

⁶G. Allan, C. Delerue, and M. Lannoo, *Phys. Rev. Lett.* **76**, 2961 (1996).

⁷M. Nayfeh, N. Rigakis, and Z. Yamani, *Phys. Rev. B* **56**, 2079 (1997); *Mater. Res. Soc. Symp. Proc.* **486**, 243 (1998).

⁸M. H. Nayfeh, O. Akcakir, G. Belomoin, N. Barry, J. Therrien, and E. Gratton, *Appl. Phys. Lett.* **77**, 4086 (2000).

⁹Z. Yamani, H. Thompson, L. AbuHassan, and M. H. Nayfeh, *Appl. Phys. Lett.* **70**, 3404 (1997); D. Andsager, J. Hilliard, J. M. Hetrick, L. H. AbuHassan, M. Plisch, and M. H. Nayfeh, *J. Appl. Phys.* **74**, 4783 (1993).

¹⁰Z. Yamani, S. Ashhab, A. Nayfeh, and M. H. Nayfeh, *J. Appl. Phys.* **83**, 3929 (1998).

¹¹Z. Yamani, A. Alaql, J. Therrien, O. Nayfeh, and M. H. Nayfeh, *Appl. Phys. Lett.* **74**, 3483 (1999).

¹²A. Yariv, *Quantum Electronics* (Wiley, New York, 1975).

¹³H. Koyama and P. Fauchet, *Appl. Phys. Lett.* **73**, 3259 (1998); H. Koyama, L. Tsybeskov, and P. Fauchet, *J. Lumin.* **80**, 99 (1999); H. Koyama and P. Fauchet, *J. Appl. Phys.* **87**, 1788 (2000); H. Koyama and P. Fauchet, *MRS* **536**, 9 (1999).